Kinetic equilibrium reconstruction of NSTX and NSTX-U plasmas using the OMFIT workflow and its impact on the transport and stability analysis

G. Avdeeva[1], K.E. Thome[1], J.W. Berkery[2], S.M. Kaye[2], J. McClenaghan[1], O. Meneghini[1], T. Odstrcil[1], S.P. Smith[1], A. Turnbull[1]

[1] General Atomics , [2] Princeton Plasma Physics Laboratory,

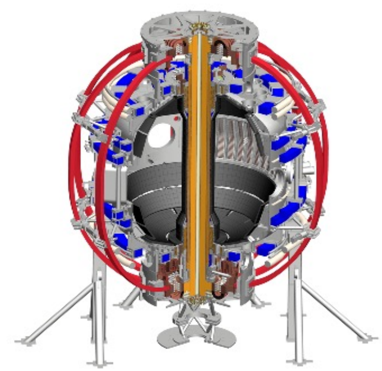

The accuracy of the equilibrium reconstruction depends on the uncertainty and quantity of imposed constraints

- EFIT equilibrium code solves the Grad-Shafranov (GS) equation:
  - minimizing the least-squares errors with imposed constraints
  - expanding the pressure and current density profiles in terms of linear basis functions

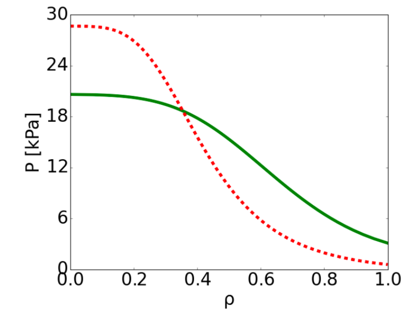

- Multiple solutions can satisfy the GS equation

Measured Signals

Computed Signals

$$\chi^2 = \sum_i \left(\frac{M_i - C_i}{\sigma_i} \right)^2$$

Measurement Uncertainty

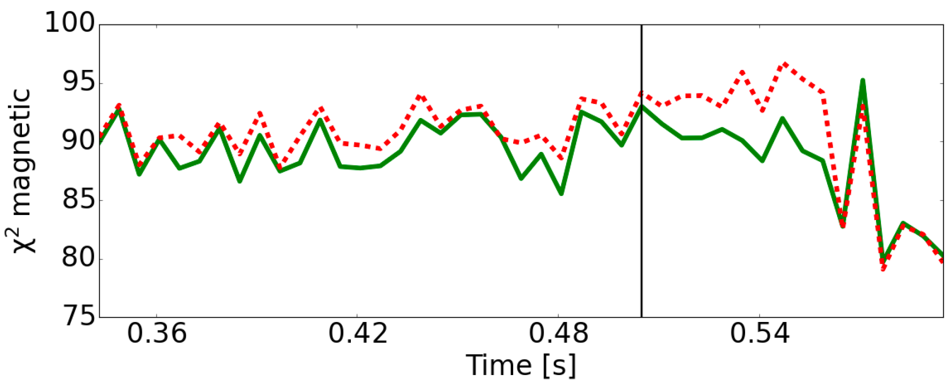

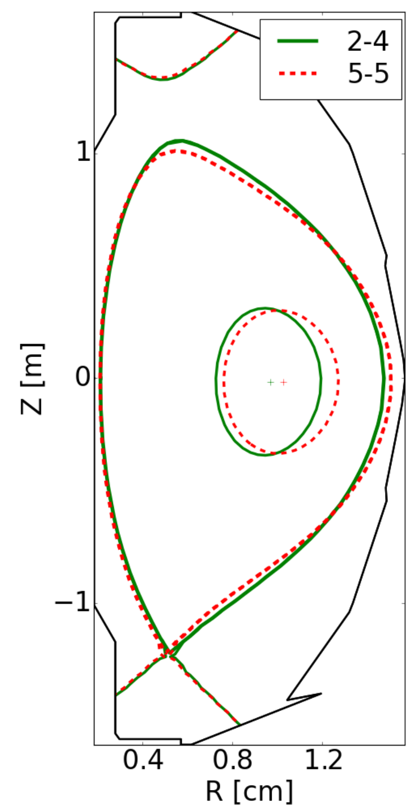

- <u>Additional internal constraints improve the fidelity of reconstruction</u>

- OMFIT workflow provides the ‘full kinetic’ equilibrium reconstruction based on magnetic, <u>MSE and transport code constraints</u>

OMFIT workflow ensures consistency between equilibrium, experimental profiles and transport code solution

- **Initial equilibrium reconstruction**: free-boundary equilibrium is obtained with the **EFIT code** based on magnetic, experimental kinetic pressure, MSE and isothermal constraints

OMFIT workflow ensures consistency between equilibrium, experimental profiles and transport code solution

- **Initial equilibrium reconstruction**: free-boundary equilibrium is obtained with the **EFIT code** based on magnetic, experimental kinetic pressure, MSE and isothermal constraints
- **Plasma profiles analysis:** fetched, mapping, filtering, averaging, fitting of experimental data with **OMFITprofiles tool**
- **Transport code simulations:** solving the current diffusion equation and calculations of the neutral beam deposition with **TRANSP+NUBEAM**

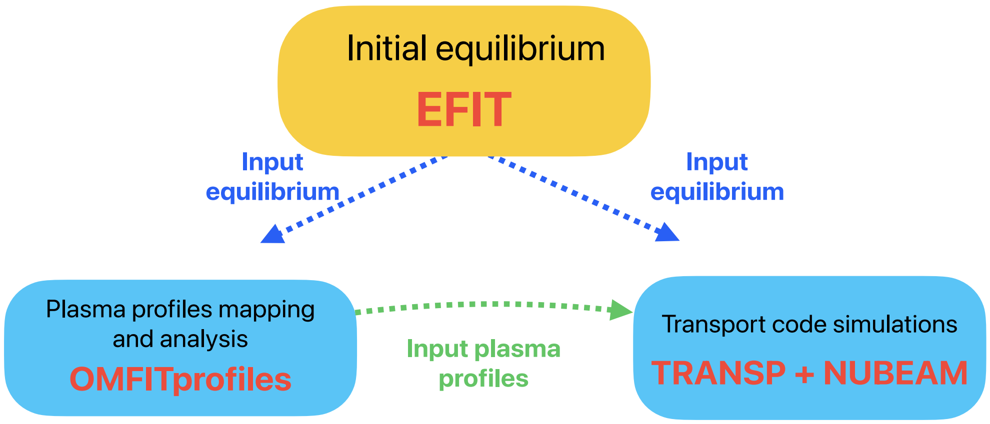

OMFIT workflow ensures consistency between equilibrium, experimental profiles and transport code solution

- **Initial equilibrium reconstruction**: free-boundary equilibrium is obtained with the **EFIT code** based on magnetic, experimental kinetic pressure, MSE and isothermal constraints
- **Plasma profiles analysis:** fetched, mapping, filtering, averaging, fitting of experimental data with **OMFITprofiles tool**
- **Transport code simulations:** solving the current diffusion equation and calculations of the neutral beam deposition with **TRANSP+NUBEAM**
- **Full kinetic equilibrium reconstruction**: equilibrium with magnetic, MSE + pressure and current constraints based on the transport code solution

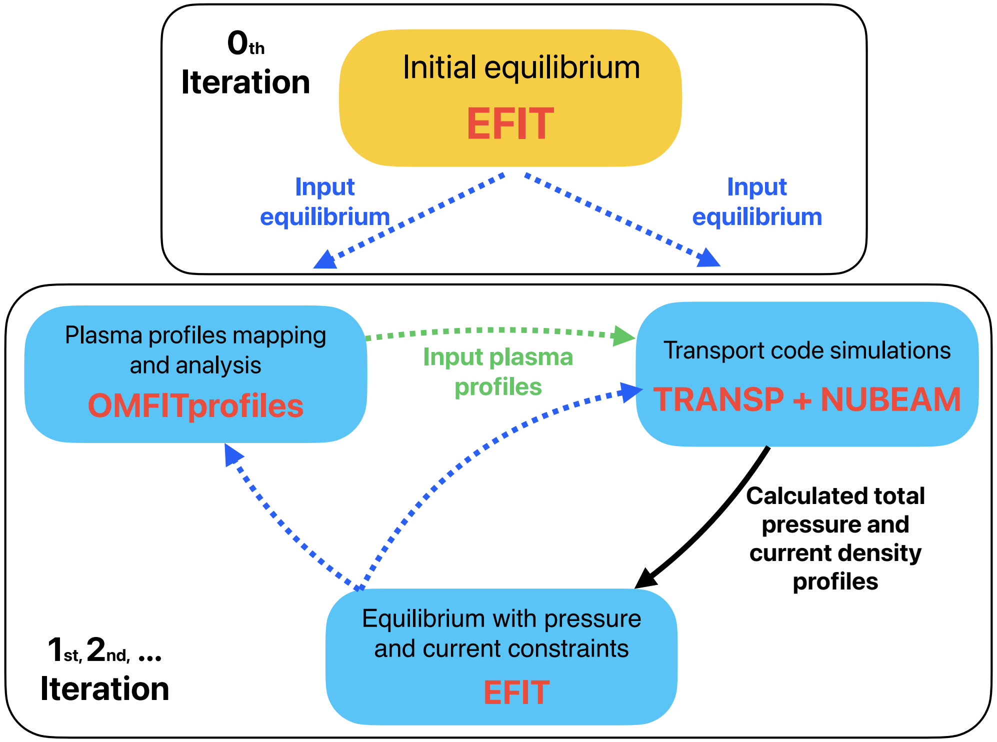

Results are demonstrated on the H-mode NSTX discharge #129017

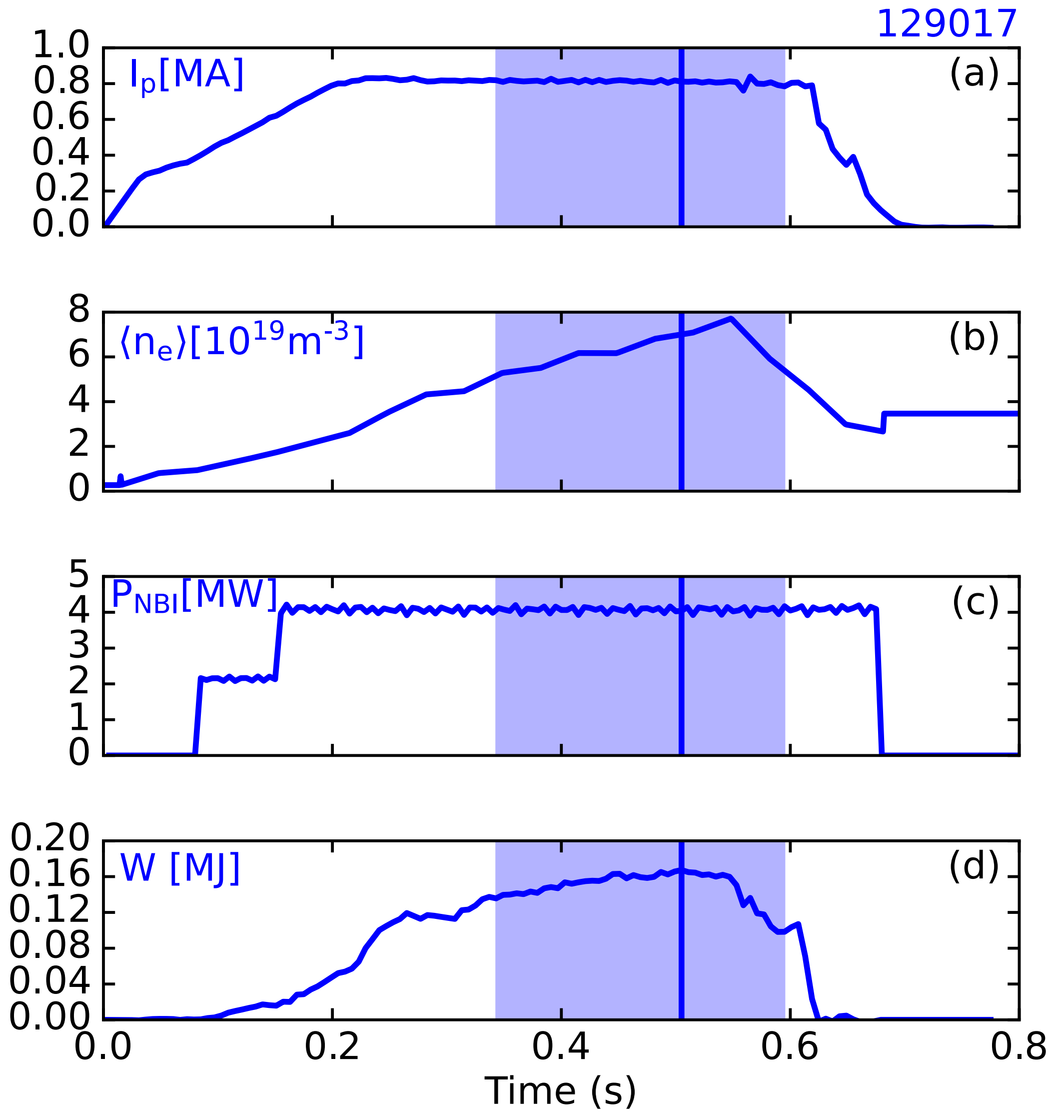

Initial equilibrium reconstruction:

experimental kinetic pressure, MSE and isothermal constrains in the OMFIT workflow

Initial equilibrium
EFIT

Magnetic data is obtained from MDS+ (k-files for EFIT01) *

Sabbagh, S. *et al.* Equilibrium properties of spherical torus plasmas in NSTX. *Nuclear Fusion* **41**, 1601–1611. ISSN: 0029-5515 (2001).

Experimental kinetic pressure constraints are based on the Thomson scattering measurements

$$P_{total} = P_{electron} + P_{ion} + P_{fast\ ion}$$
$$= 3 \cdot n_e \cdot T_e$$

- Large error bars are due to unknown fast ion pressure
- Polynomial representation for pressure and current basis functions + boundary conditions P'(0)=0; (FF'(1))'=0
- **Solution strongly depends on the polynomial order of basis function**

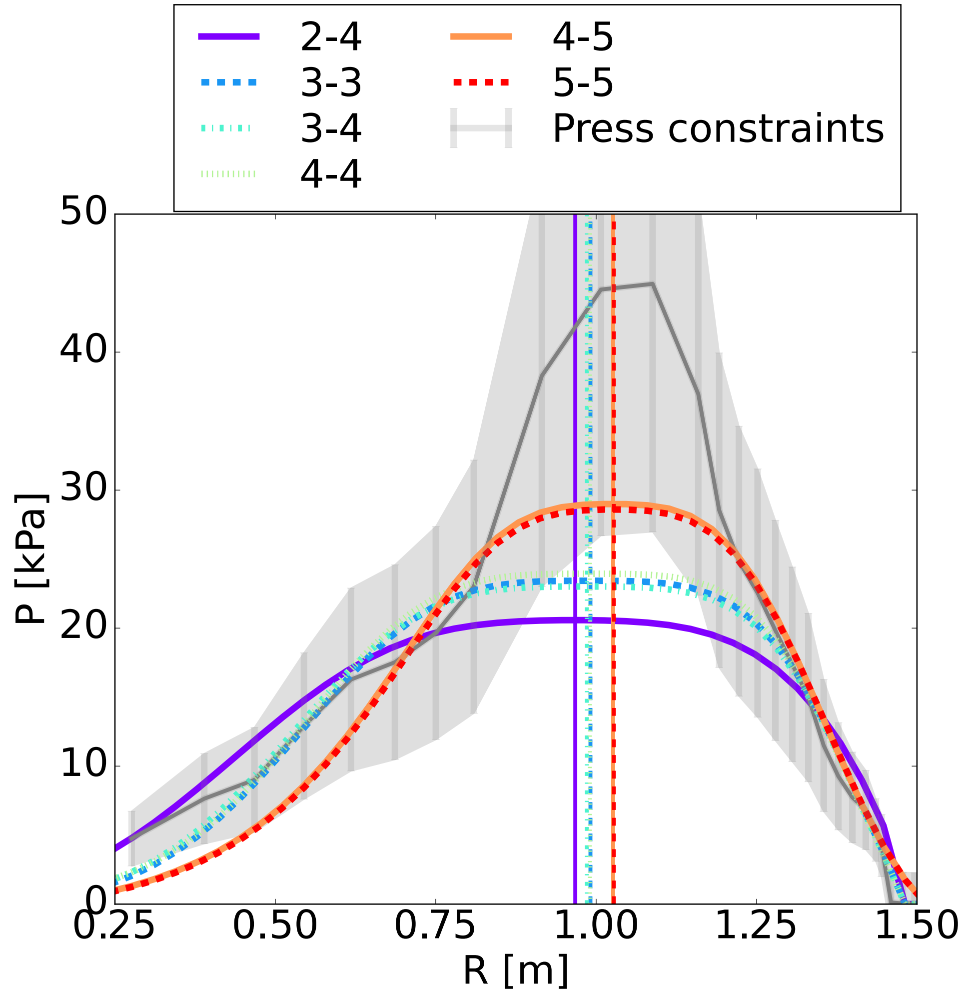

Motional Stark effect (MSE) measurements are applied for the current density profile constraints

- MSE constraints are applied with a high weight (10 times higher compared to other constraints)
- Removing the boundary conditions for the basis functions noticeably reduces the χ^2 error of MSE data
- MSE measurements are not accurate at the edge region ($\rho > 0.7$) → need transport code constraints

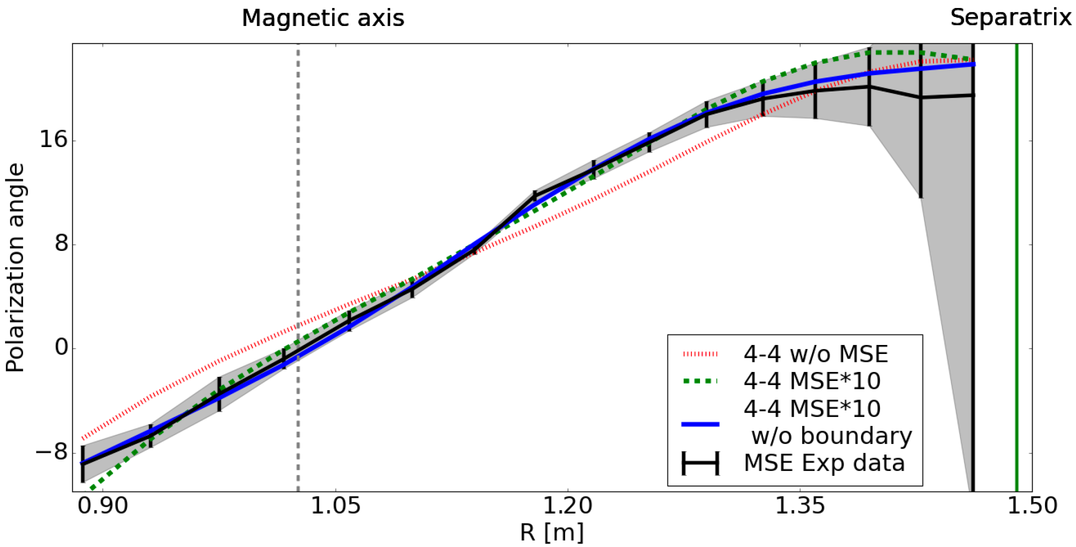

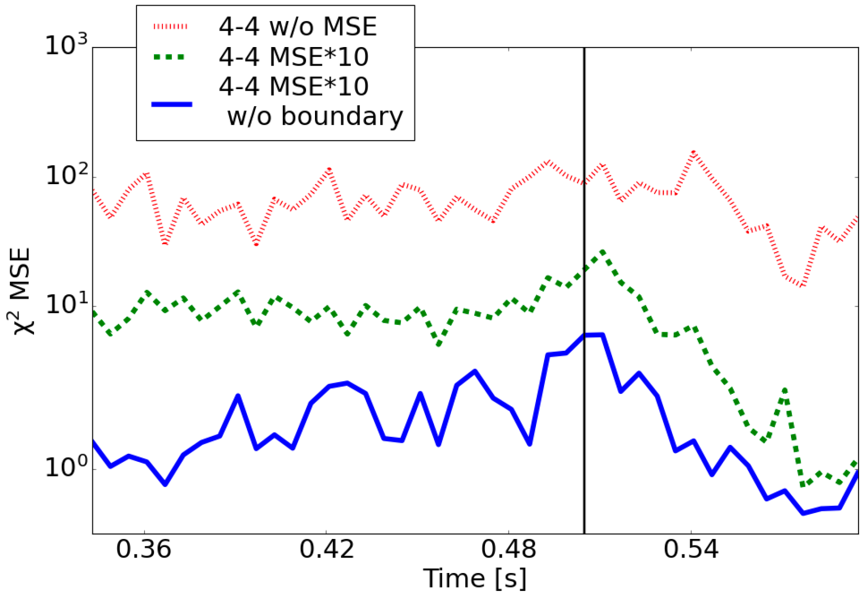

Motional Stark effect (MSE) measurements are applied for the current density profile constraints

- Reconstructed plasma profiles with MSE constraints are more peaked and the axis location is shifted outward

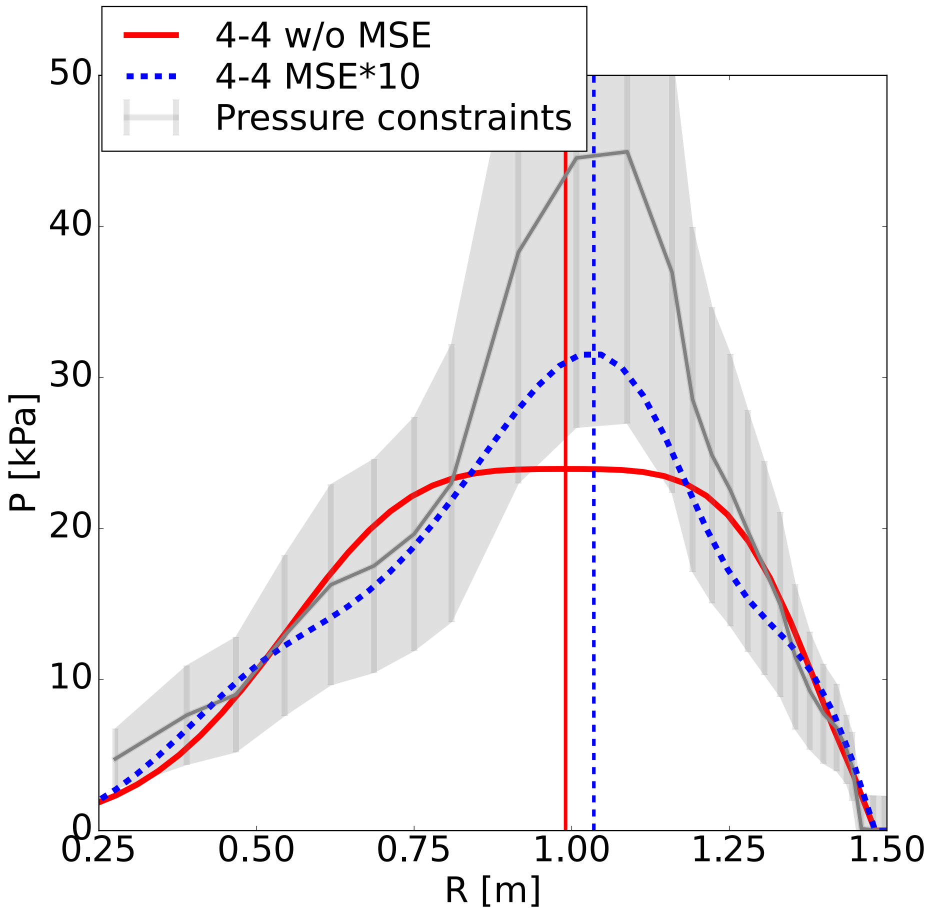

- MSE constraints are consistent with magnetic diagnostics

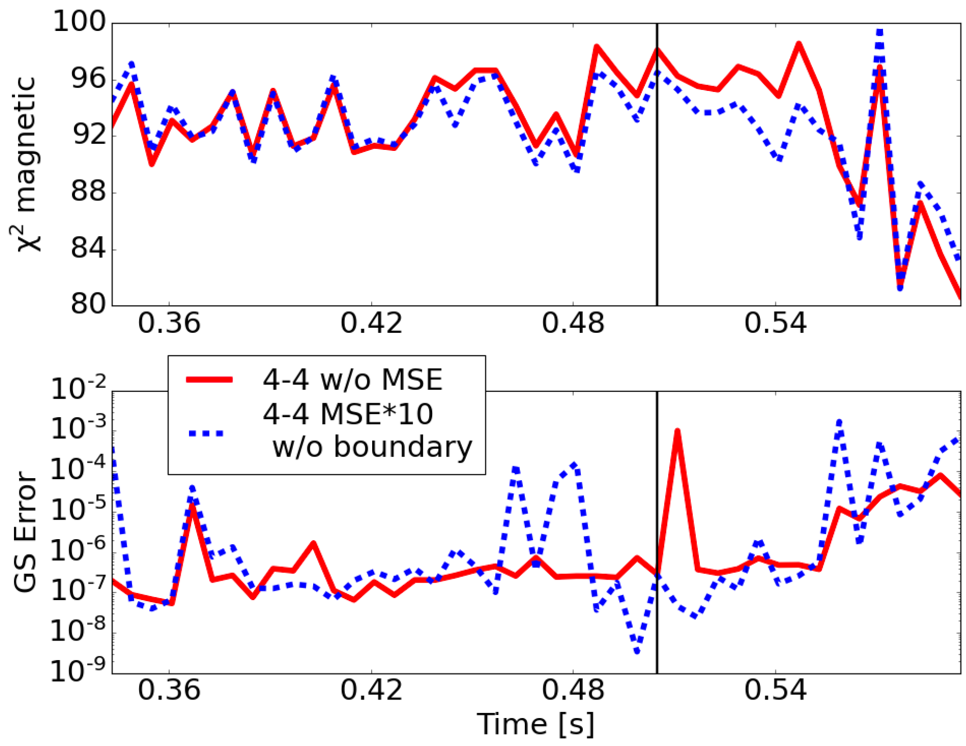

Isothermal constraints are applied for symmetrization of T_e and n_e measurements on flux coordinates

- Constraints are based on T_e measurements and the assumption of fast parallel heat conductivity.
- The magnetic axis location determining the center of the profile is defined based on the MSE data.

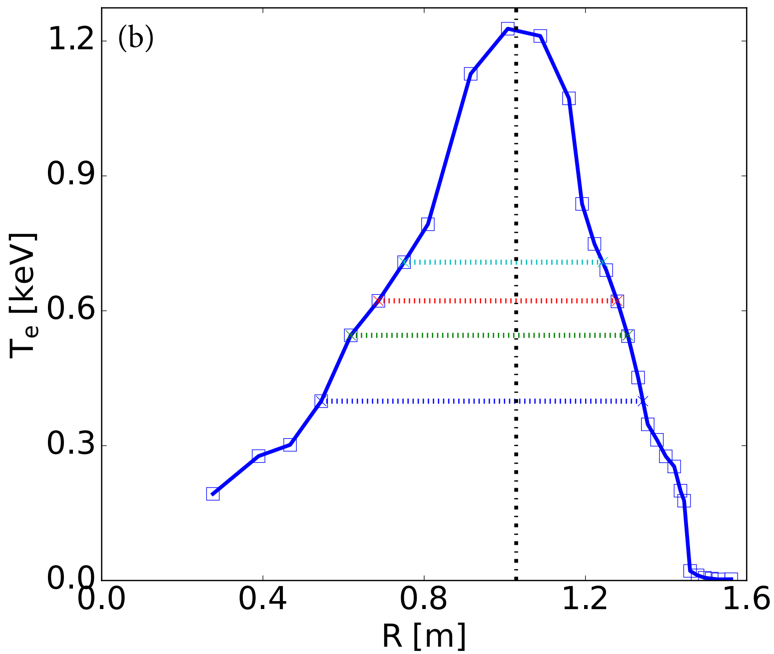

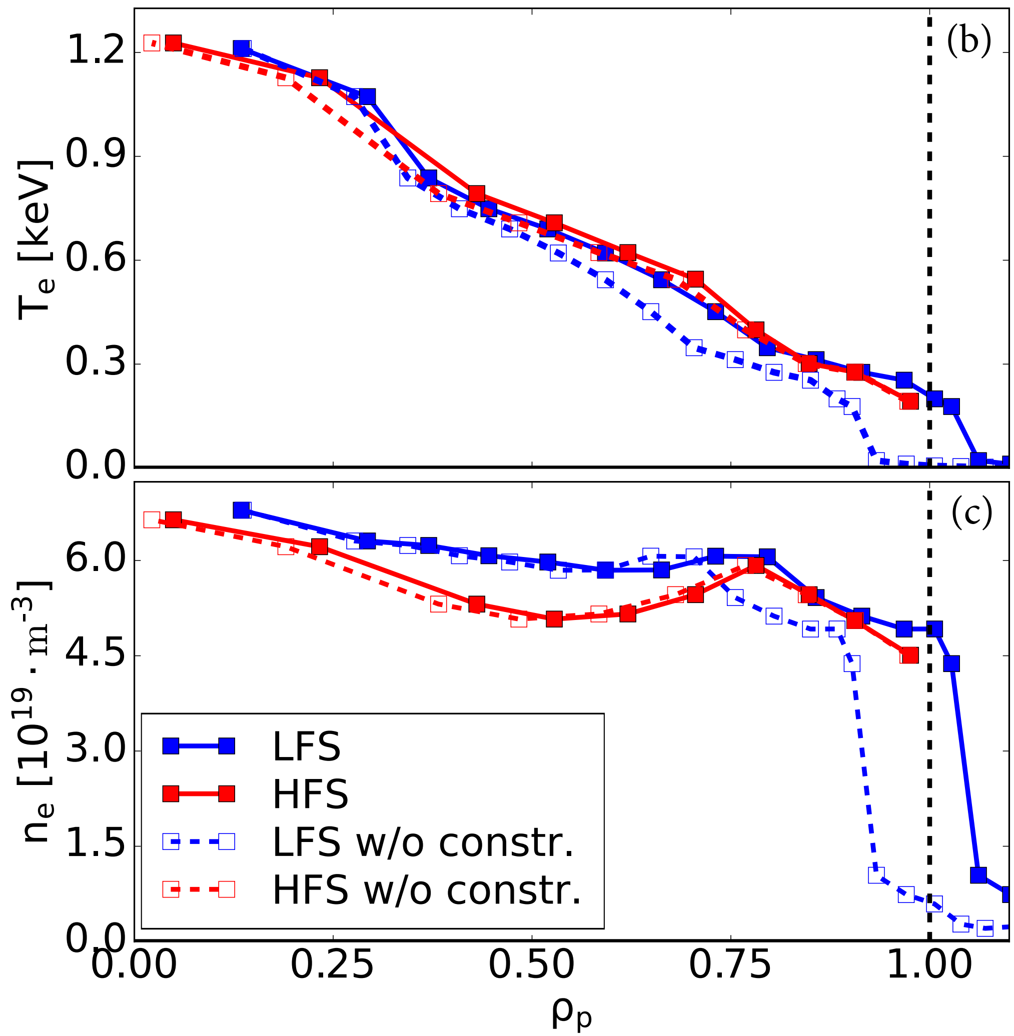

Experimental data analysis:

Influence of a choice of the fitting method and equilibrium reconstruction on plasma profiles

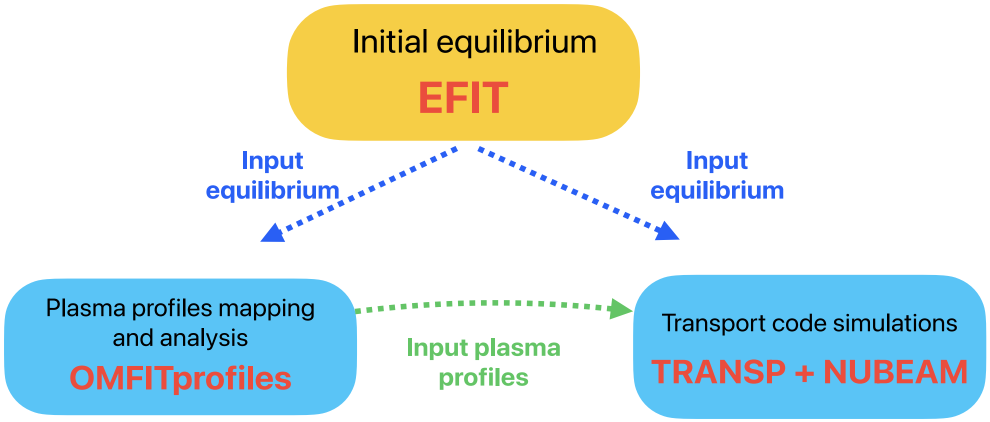

Mapping on the equilibrium with more constraints leads to higher pedestal plasma parameters at $\rho \geqslant 0.8$

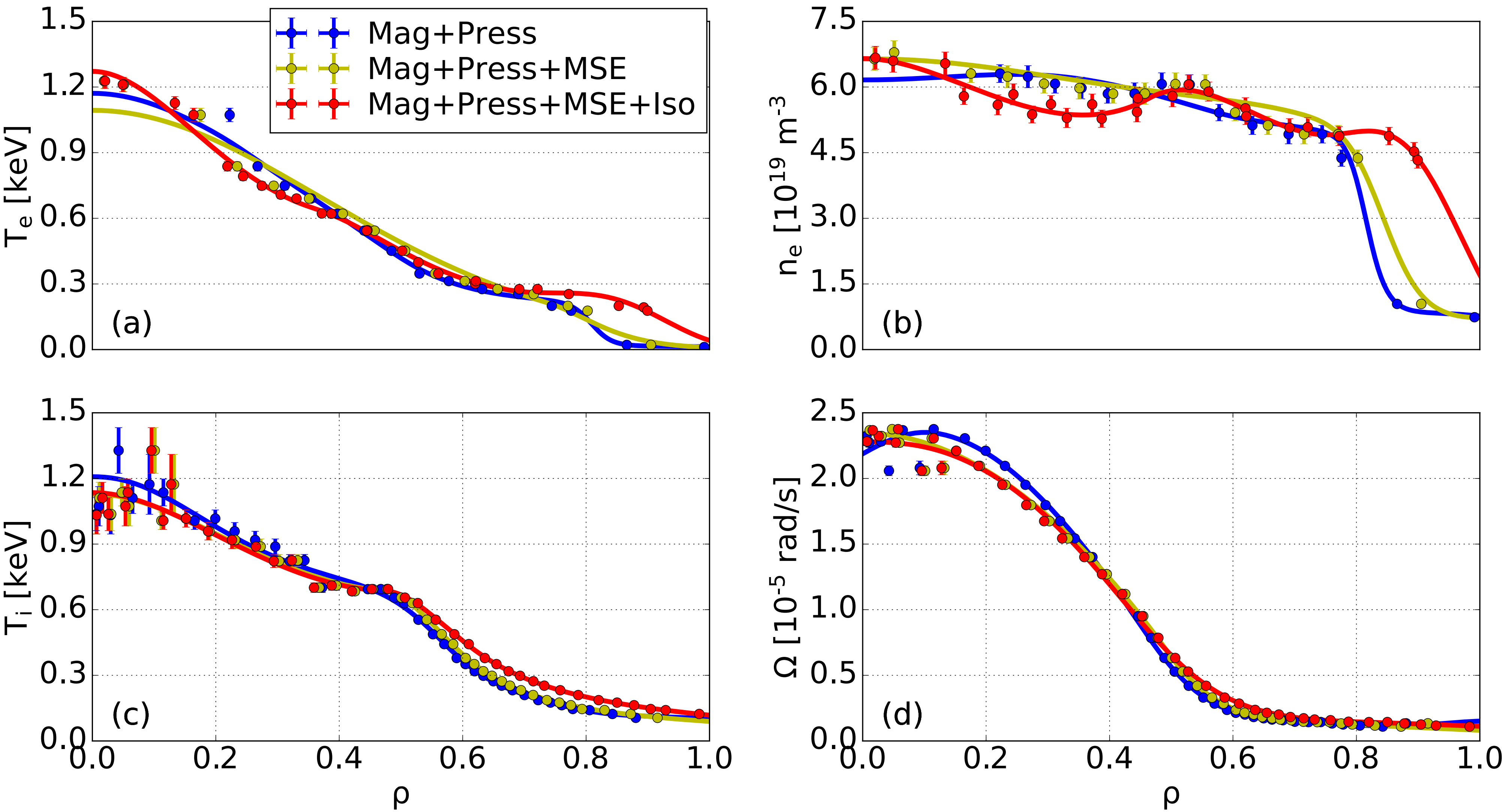

The biggest impact of the choice of the fitting method is on the plasma density and temperature profiles

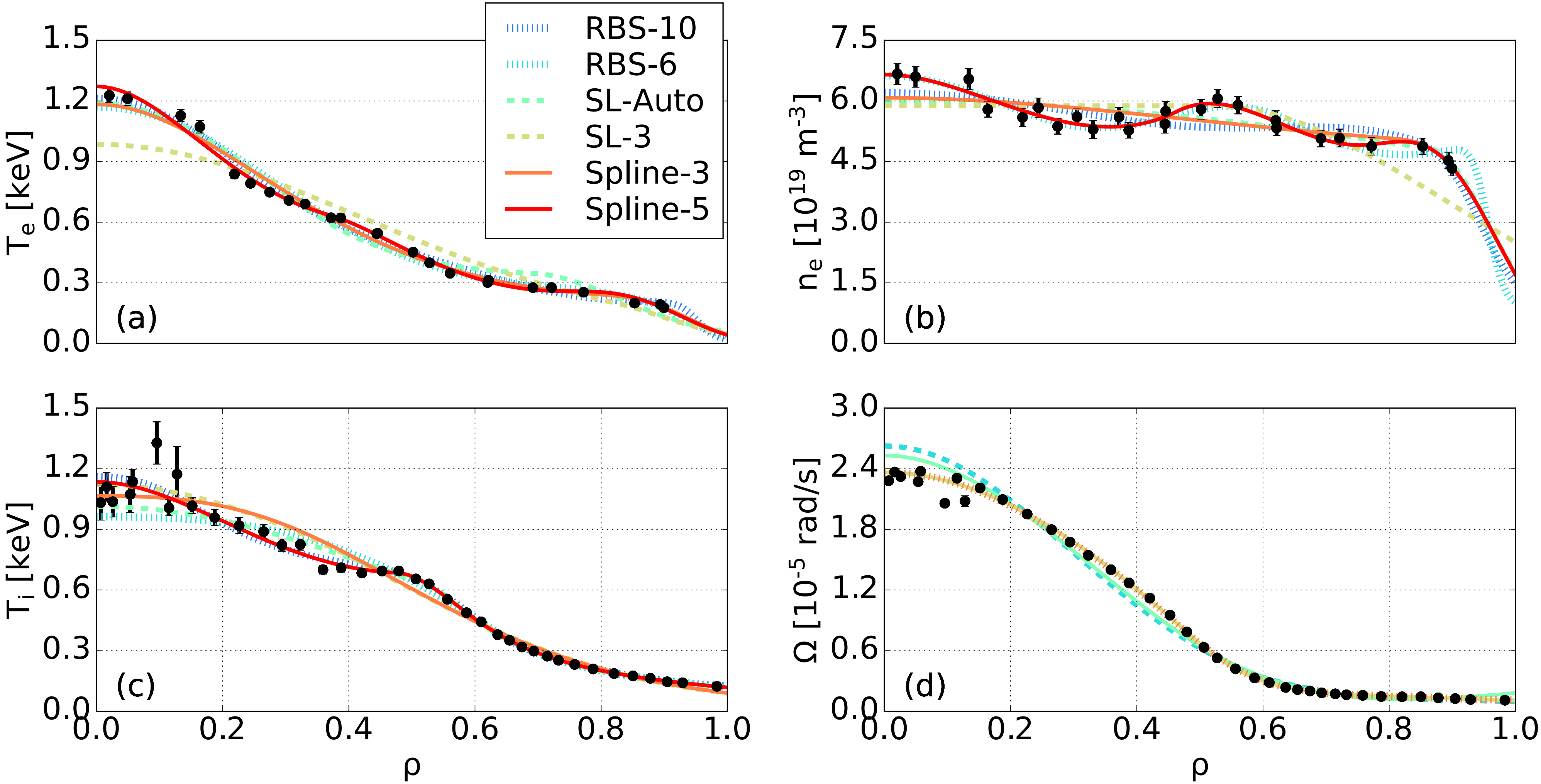

The choice of the fitting method more strongly affects the profiles in the core region; equilibrium – at the edge region

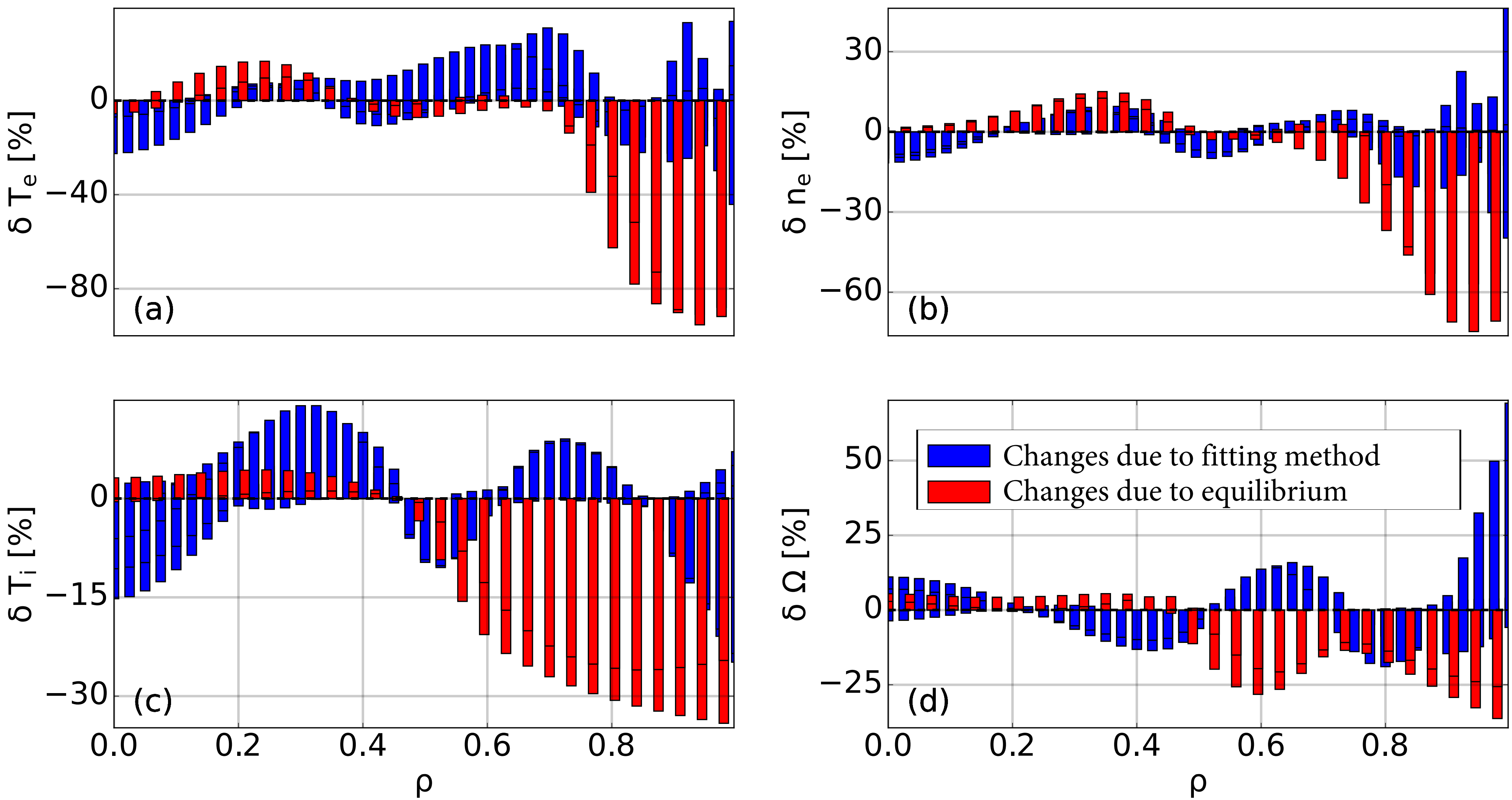

Transport code simulations:

Calculations of total pressure and current density profiles

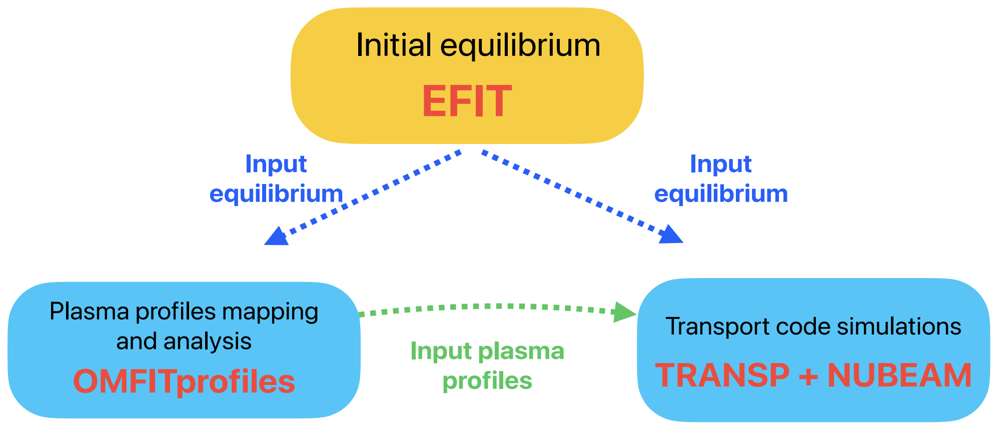

The fast-ion pressure resulting from the neutral beam injection is calculated with the TRANSP+NUBEAM

- The fast ion pressure contribution can be up to 60% of the total plasma pressure on the axis.

- Calculations of the fast ion density are not sensitive to changes in mapping and equilibrium, however the thermal pressure is sensitive.

- Results are validated by comparison of calculated and measured neutron rates, if necessary the anomalous fast ion diffusion is adjusted to get a better agreement.

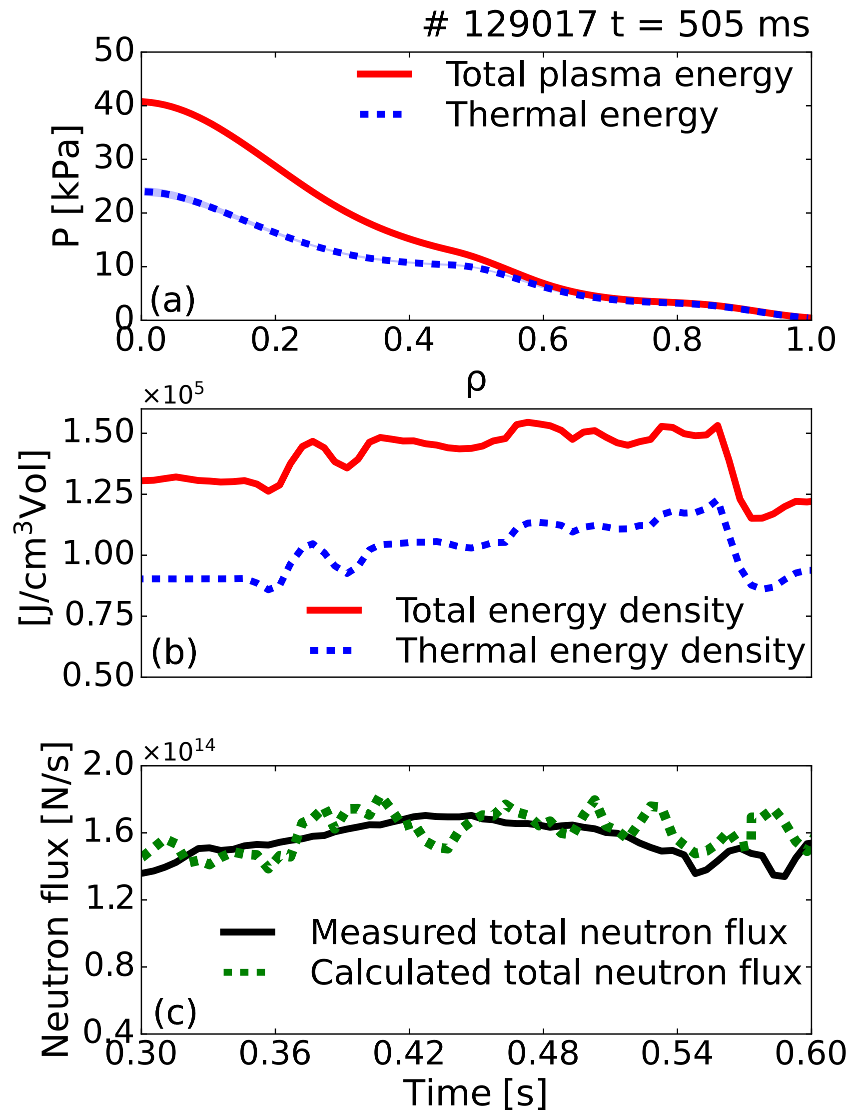

The current density profile is calculated based on the solution of the magnetic flux diffusion equation

- The bootstrap current and the resistivity are calculated according to the Sauter model.

- The solution is validated by comparison of calculated and measured surface voltage, as well as experimental and synthetic MSE signals.

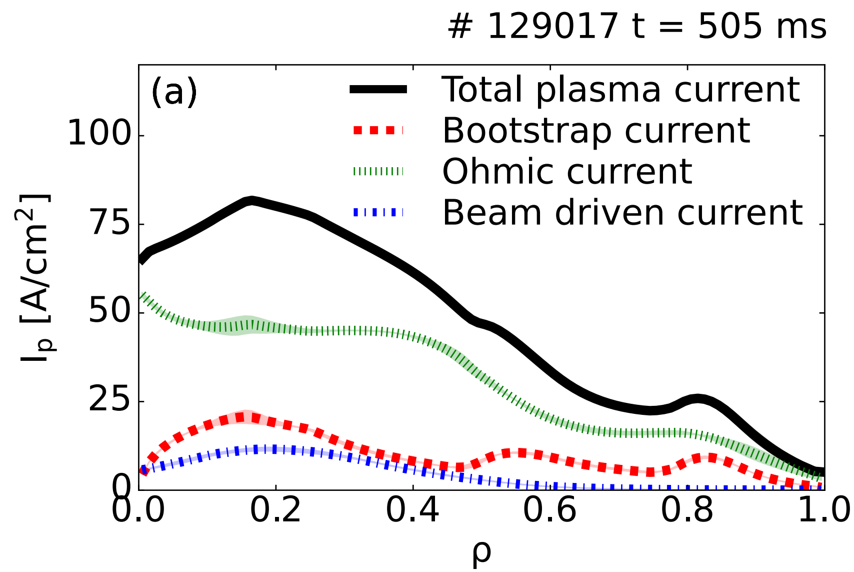

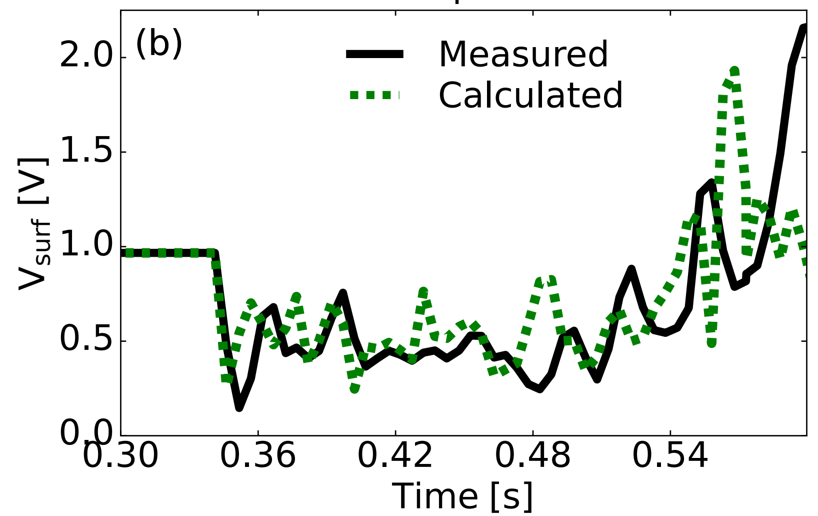

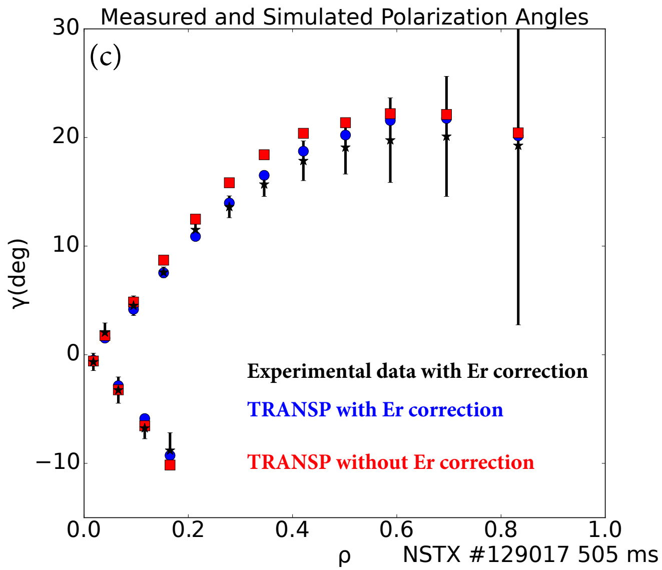

Full kinetic equilibrium:

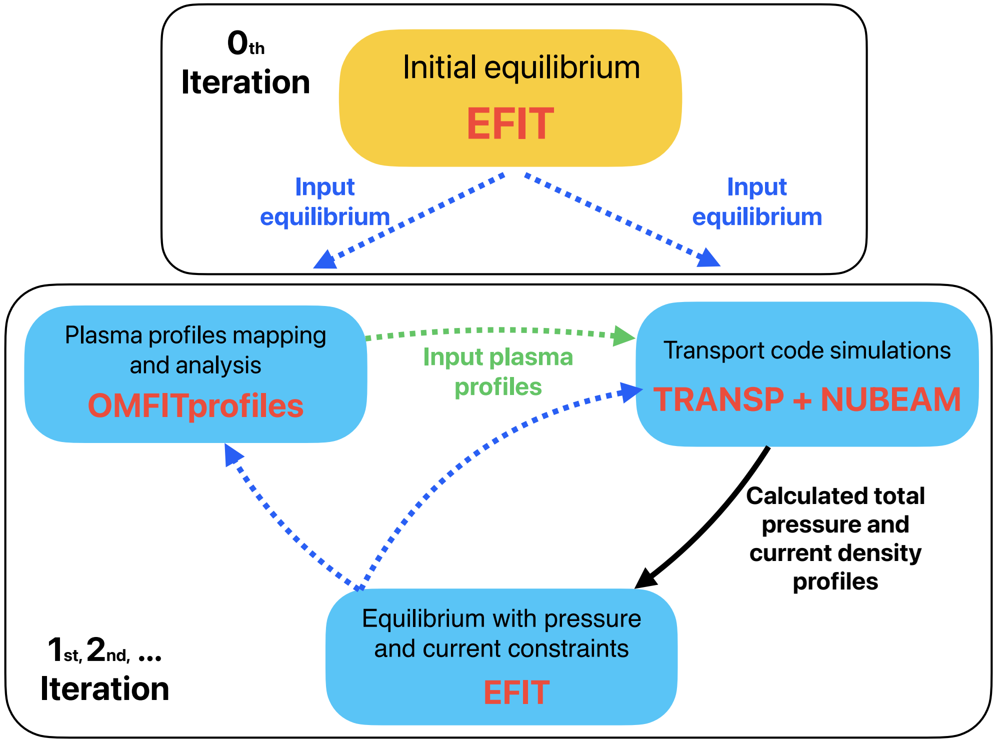

The solution with transport code constraints (‘Full kinetic’) has higher gradients at the plasma edge

- A tension spline representation is used for the pressure and current basis functions

- The uncertainty of the pressure profiles is established as 30% of the thermal pressure and 50% of the fast ion pressure.

- The current density constraints obtained from the transport code are applied only at the pedestal region ρ > 0.7 and with a low weight.

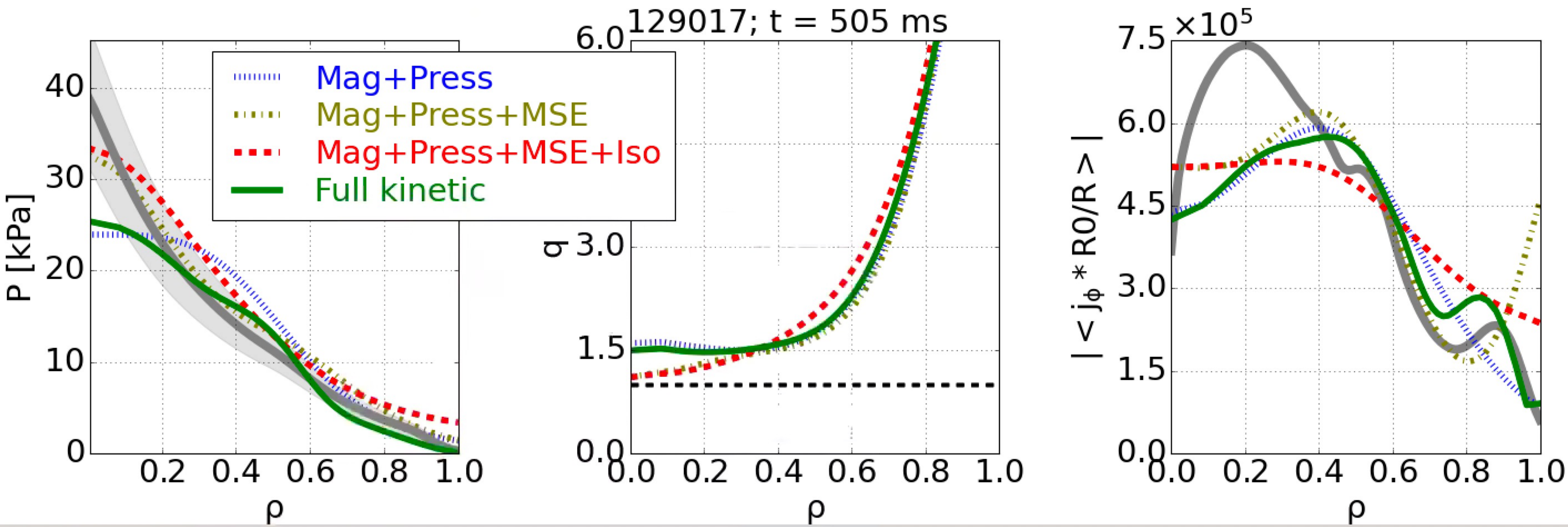

The sensitivity of the solution to the choice of the basis functions decreases with increased number of the constraints

Sensitivity of the solution to the polynomial order or spine tension variations for basis functions

	Case 1	Case 2	Case 3	Case 4
	Mag + Press	Mag + Press + MSE	Mag + Press + MSE + Iso	Mag + MSE + Transport code
ΔR_{axis} [cm] - magnetic axes location	4.4	0.52	0.04	0.25
ΔR_{LCFS} [cm] - separatrix location at the midplane	2.2	0.82	0.71	0.56
ΔI_p [MA] - total plasma current	0.01	0.01	0.02	< 0.01
Δl_i - inductance	0.19	0.06	0.05	0.02
ΔW_{plasma} [MJ] - stored energy	0.02	0.01	0.01	< 0.01
Δq_0 - safety factor on axis	0.91	0.12	0.09	0.12
ΔP_{max} [kPa] - maximum pressure	6.2	1.12	1.03	0.51

Impact on the stability and transport analysis

The accuracy of the equilibrium affects the results of linear CGYRO simulations

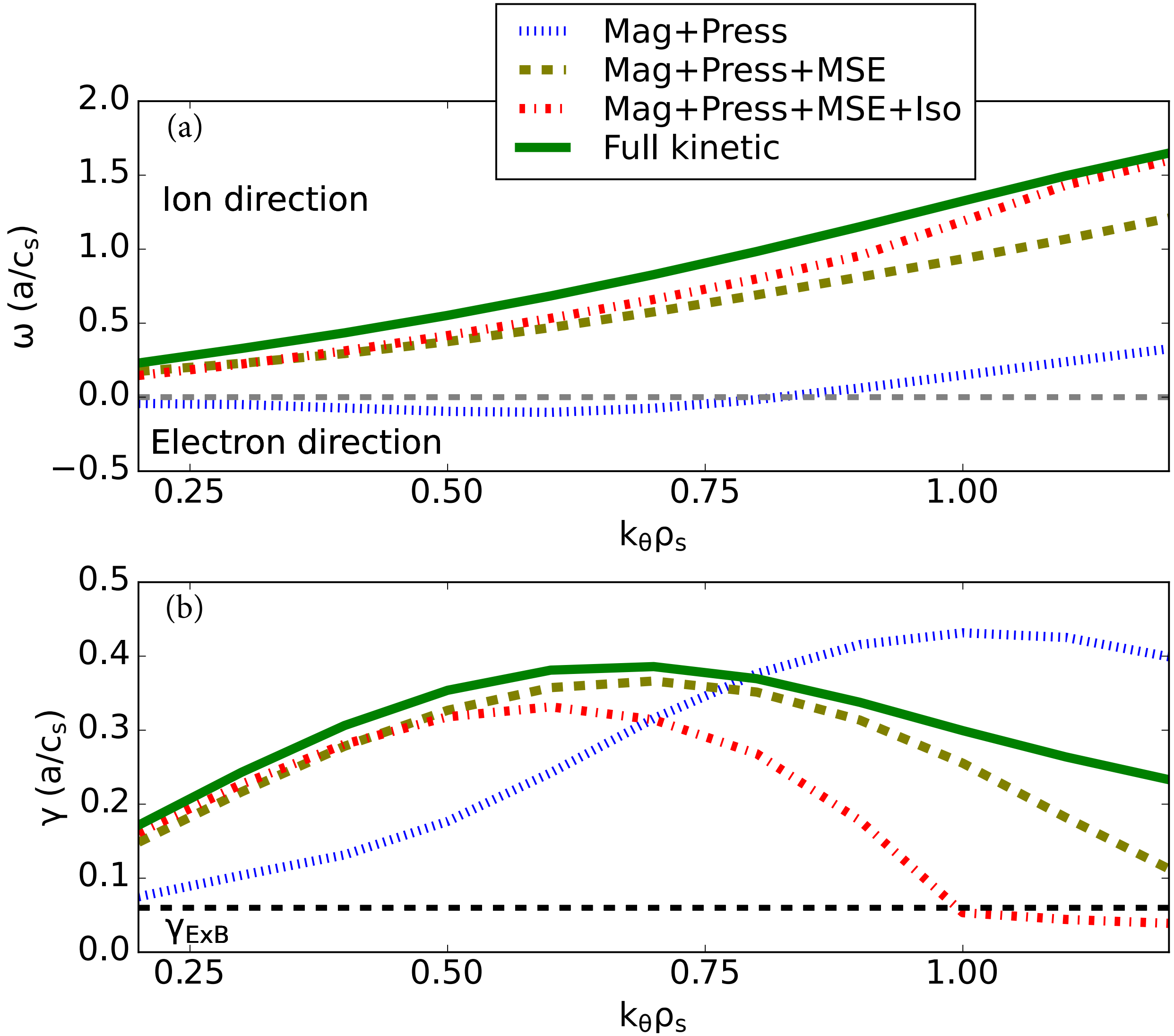

GATO MHD stability threshold is different for equilibria with different number of constraints

The scaling is done by resetting the toroidal field b_{tor} to b_{new}

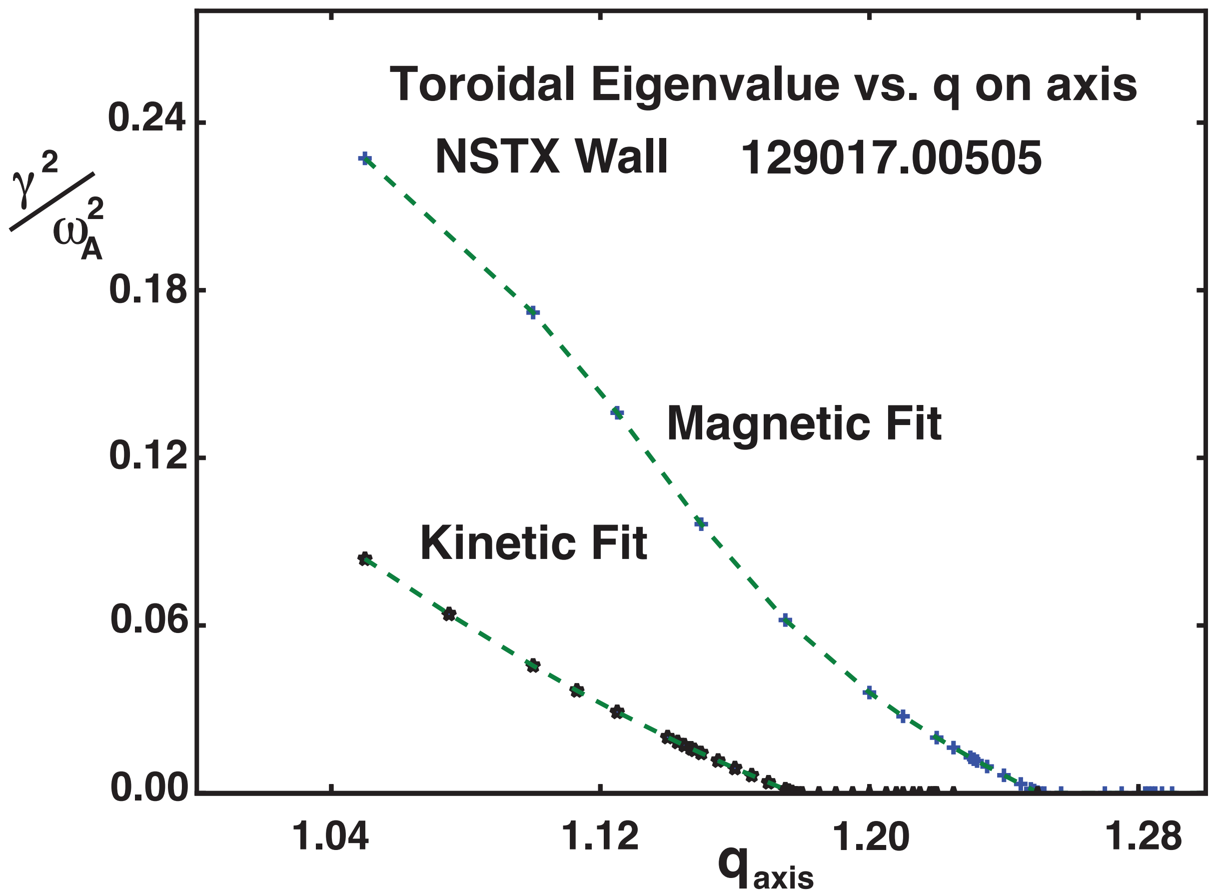

q0 Magnetic – 1.5 +/- 0.9

q0 Kinetic – 1.52 +/- 0.1

The same OMFIT workflow can be applied to the NSTX-U discharges

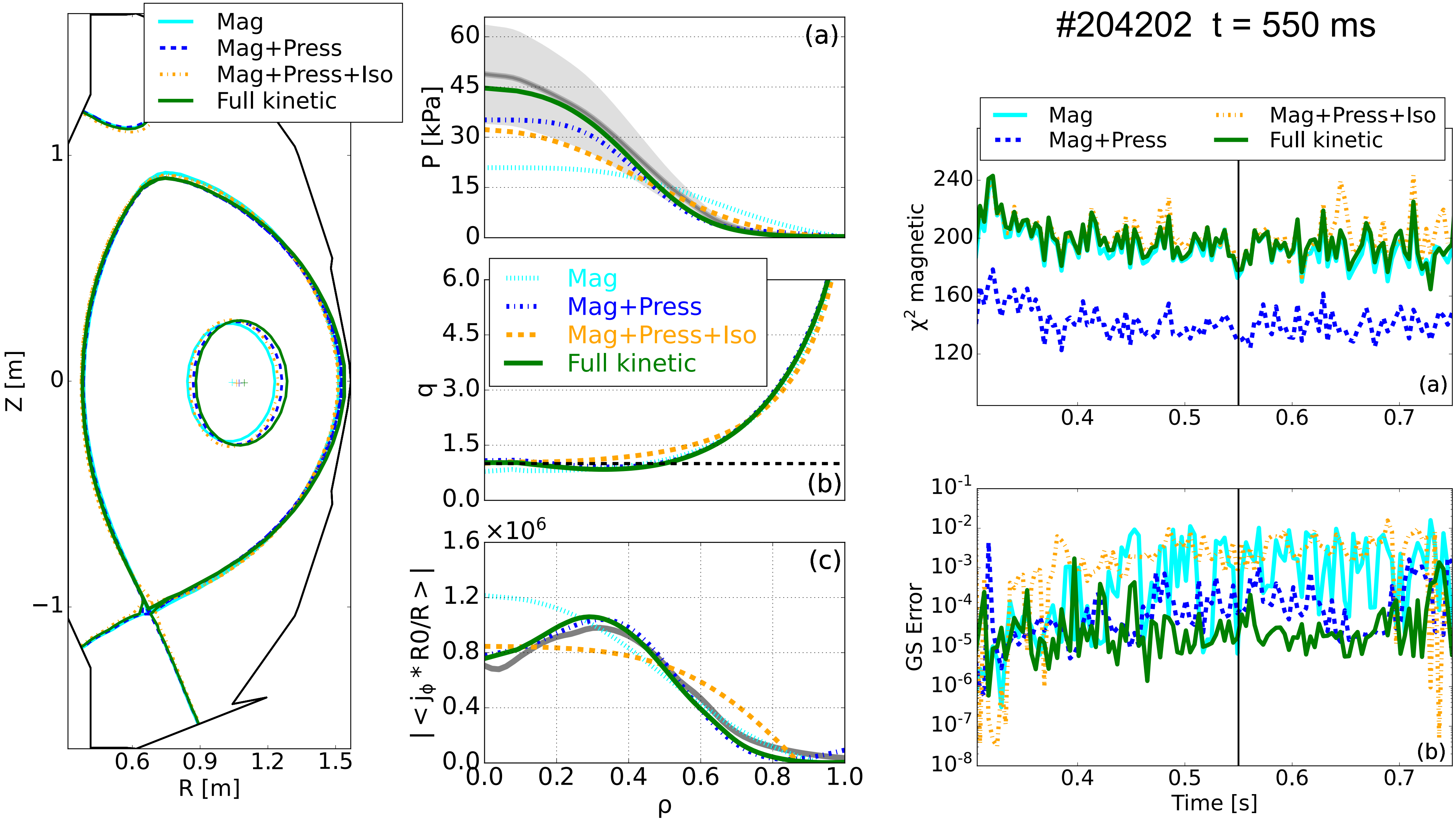

OMFIT kineticEFITtime workflow is adapted for NSTX/NSTX-U specific data

- The EFIT equilibrium solver is integrated with experimental data analysis procedures and subsequent TRANSP transport simulations to enhance the accuracy of the reconstruction

- More peaked pressure profiles are obtained with the MSE constraints and the axis location corresponding to the center of the profile is shifted outwards.

- The solution with transport code constraints has significantly higher gradients at the plasma edge

- The variations of the magnetic axis and boundary location are reduced to several millimeters and the sensitivity of the safety factor on axis is reduced by a factor of ten with increased number of constraints

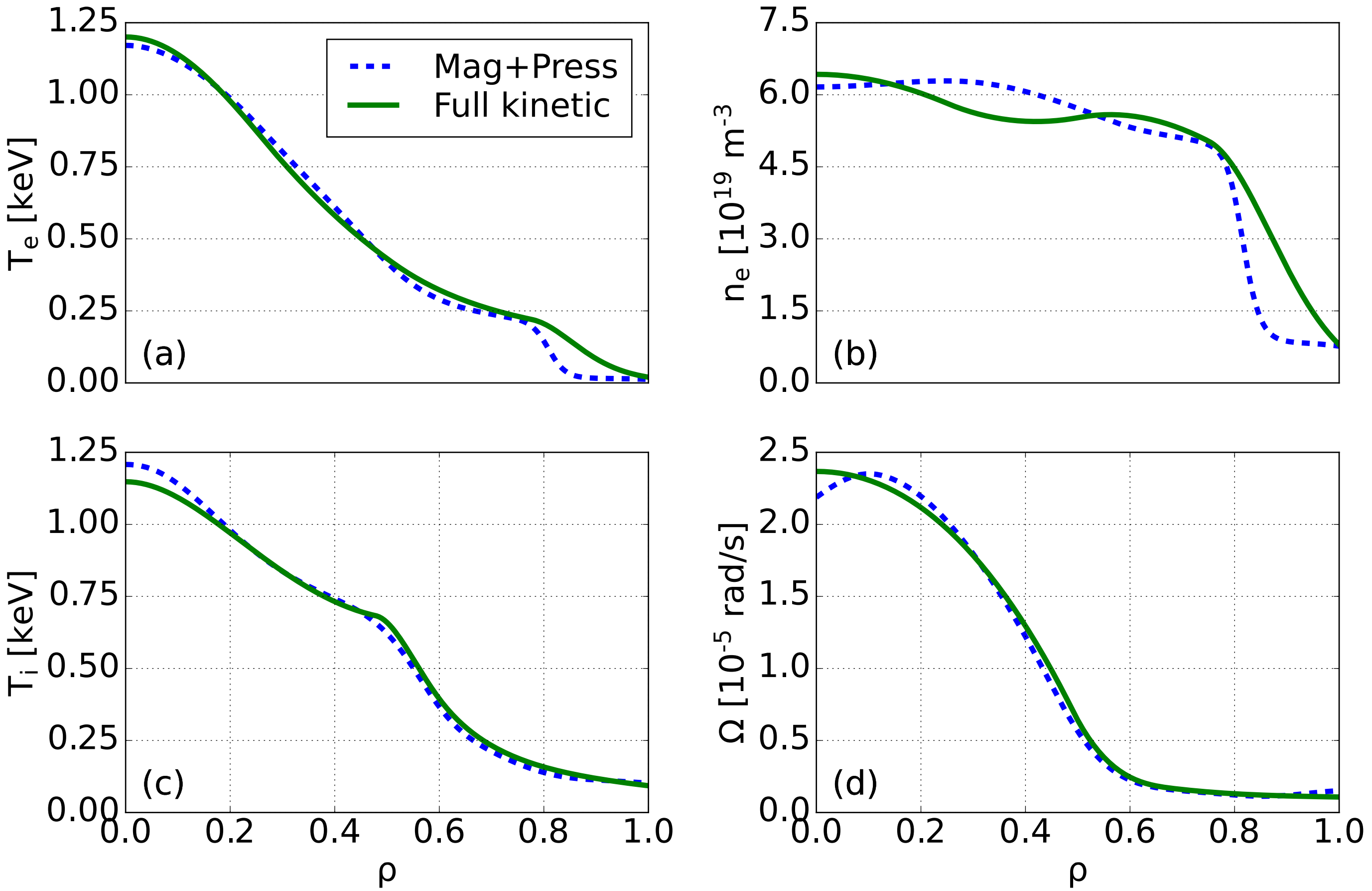
Mag+Press
Full kinetic
T_e [keV]
n_e [10^{19} m^{-3}]
T_i [keV]
Ω [10^{-5} rad/s]
(a)
(b)
(c)
(d)
ρ
ρ

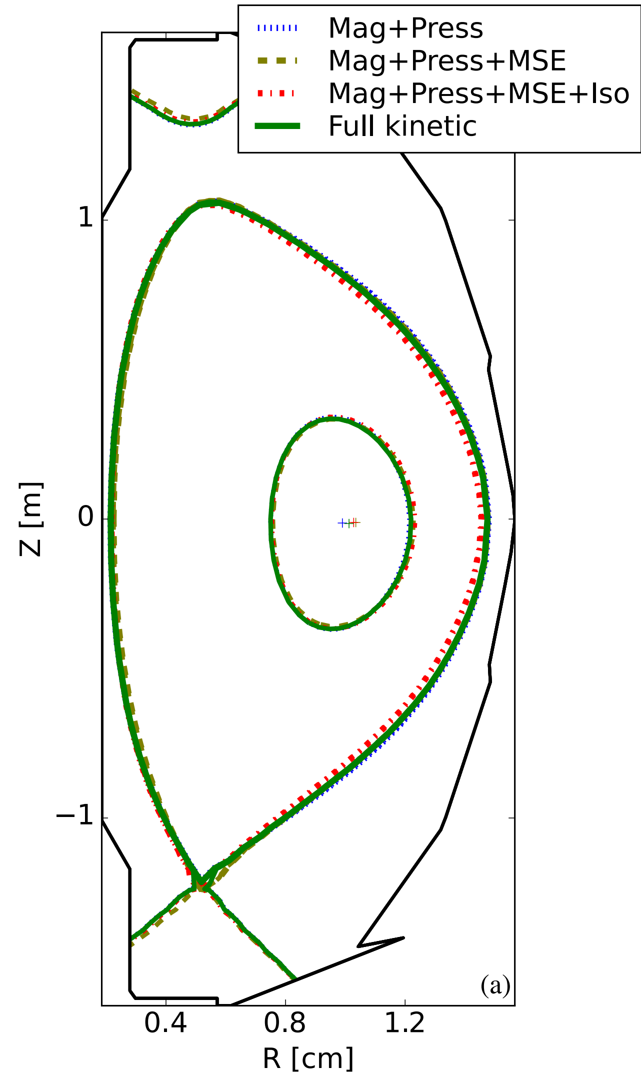
Mag+Press
Mag+Press+MSE
Mag+Press+MSE+Iso
Full kinetic
Z [m]
R [cm]
(a)

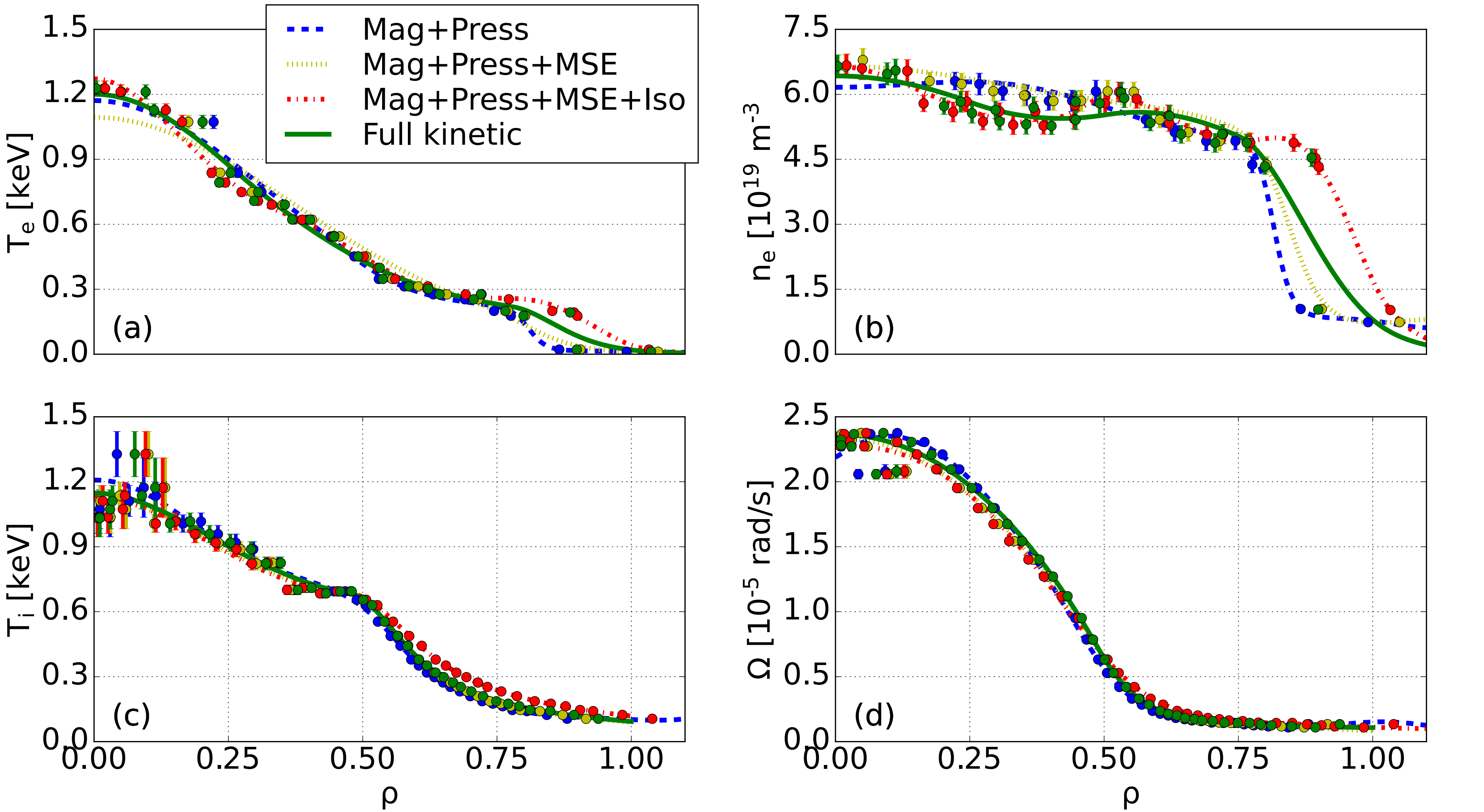

Mag+Press
Mag+Press+MSE
Mag+Press+MSE+Iso
Full kinetic
T_e [keV]
n_e [10^{19} m^{-3}]
T_i [keV]
Ω [10^{-5} rad/s]
ρ
ρ
(a)
(b)
(c)
(d)

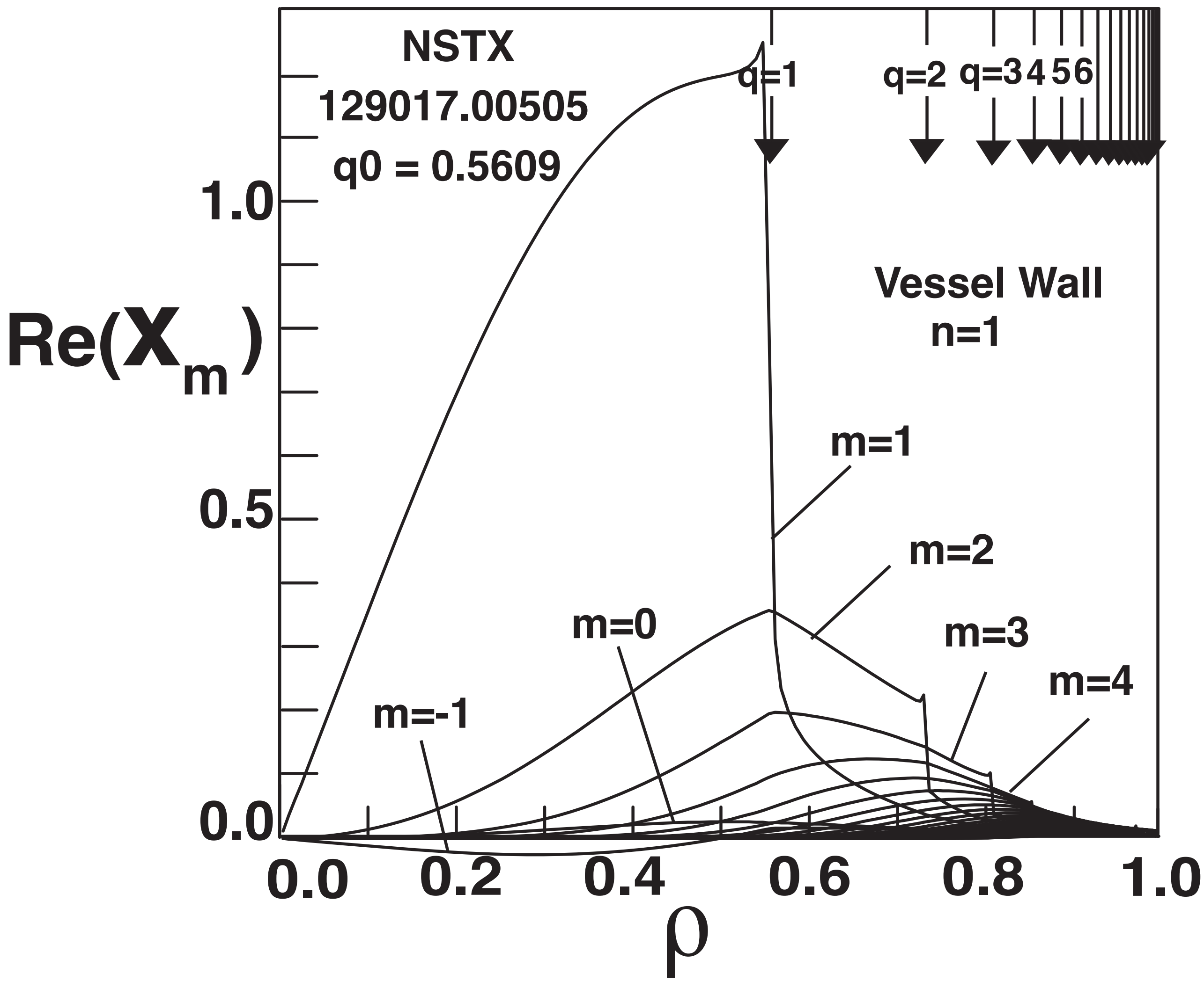
NSTX
129017.00505
q0 = 0.5609
q=1
q=2
q=3 4 5 6
1.0
0.5
0.0
Re(X_m)
Vessel Wall
n=1
m=1
m=2
m=0
m=3
m=4
m=-1
0.0
0.2
0.4
0.6
0.8
1.0
ρ

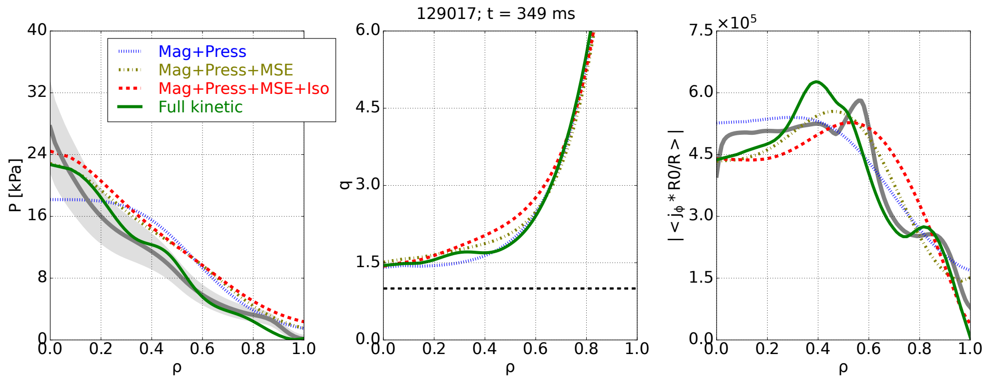
129017; t = 349 ms
Mag+Press
Mag+Press+MSE
Mag+Press+MSE+Iso
Full kinetic
P [kPa]
q
| < j_ϕ * R0/R > |
ρ

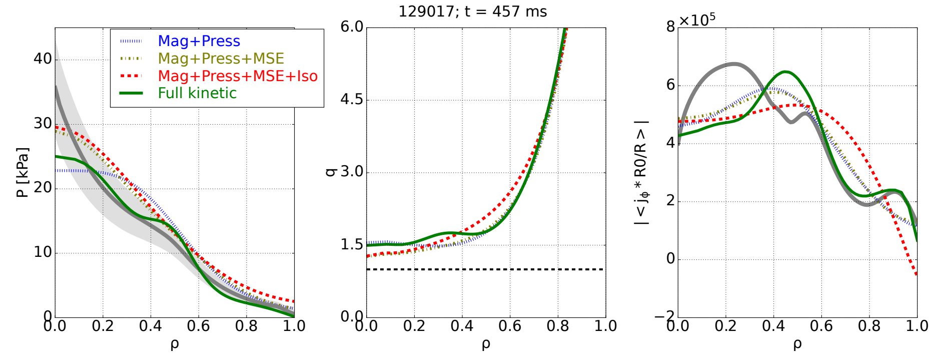
129017; t = 457 ms
Mag+Press
Mag+Press+MSE
Mag+Press+MSE+Iso
Full kinetic
P [kPa]
q
| < j_ϕ * R0/R > |
ρ

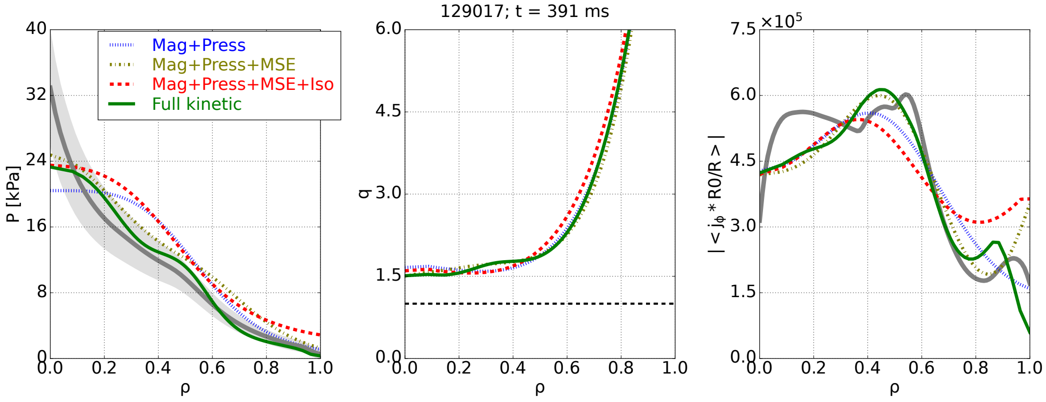
129017; t = 391 ms
Mag+Press
Mag+Press+MSE
Mag+Press+MSE+Iso
Full kinetic
P [kPa]
q
| < j_ϕ * R0/R > |
ρ

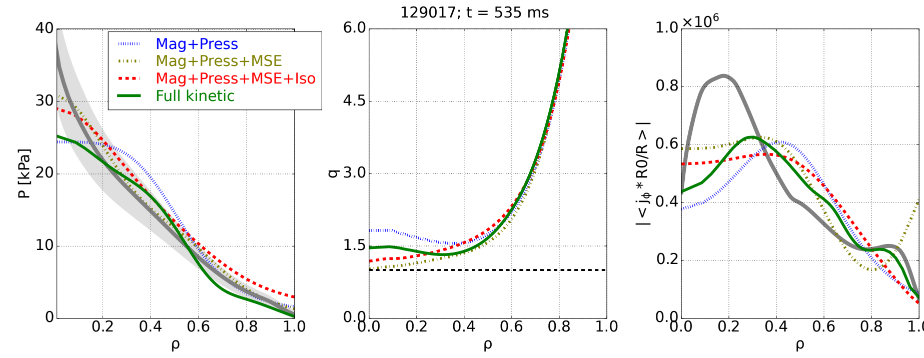
129017; t = 535 ms
Mag+Press
Mag+Press+MSE
Mag+Press+MSE+Iso
Full kinetic
P [kPa]
q
| < j_ϕ * R0/R > |
ρ

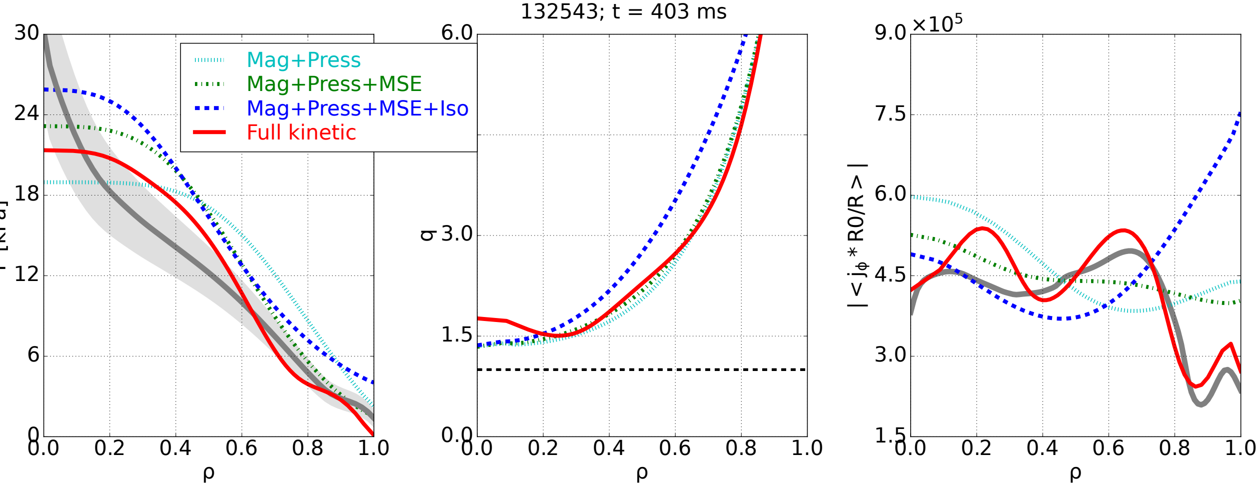
132543; t = 403 ms
Mag+Press
Mag+Press+MSE
Mag+Press+MSE+Iso
Full kinetic
ρ
q
| < j_ϕ * R0/R > |
×10^5

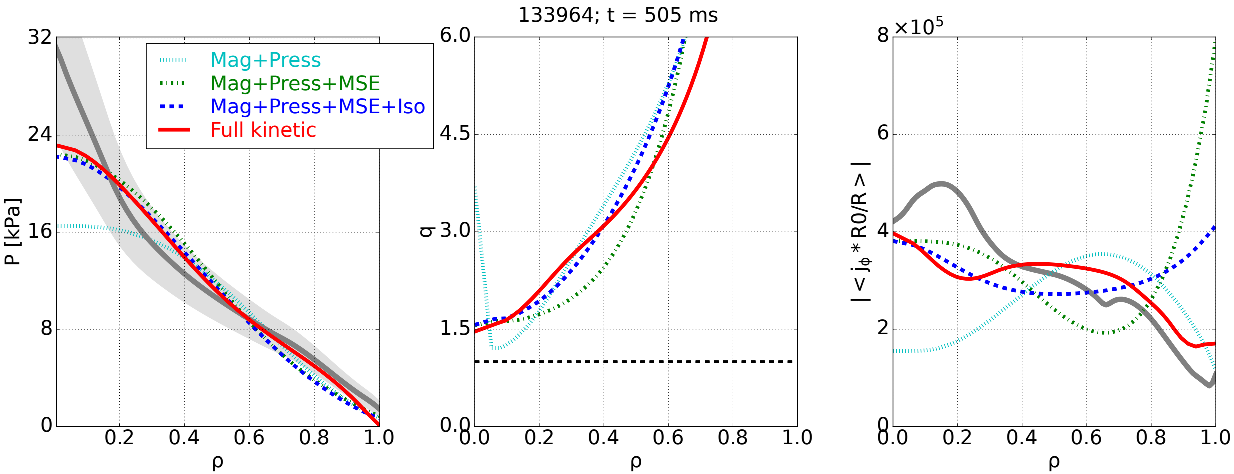
133964; t = 505 ms
Mag+Press
Mag+Press+MSE
Mag+Press+MSE+Iso
Full kinetic
P [kPa]
ρ
q
| < j_ϕ * R0/R > |
×10^5